Geologie en Mijnbouw **76:** 73–82, 1997.

How far between Iran and Eurasia was the Turan plate during Triassic–Jurassic times?

M.M. Lemaire[1], M. Westphal[1], E.L. Gurevitch[2], K. Nazarov[3], H. Feinberg[4] & J.P. Pozzi[4]

[1] *Ecole et Observatoire des Sciences de la Terre, UMR 7516, 5 rue R. Descartes, 67084 Strasbourg Cedex, France (mlemaire@eost.u-strasbg.fr; mwestphal@eost.u-strasbg.fr);* [2] *V.N.I.G.R.I., Liteiny 39, 191104 St Petersburg, Russia (gur@oloy.spb.su);* [3] *Institute of Geology, Academy of Sciences, Ashkhabat, Turkmenistan;* [4] *Ecole Normale Supérieure, URA 1316, Dept. de Géologie, 24 rue Lhomond, 75231 Paris 05, France (feinberg@magnetit.ens.fr; pozzi@magnetit.ens.fr)*

Received 3 September 1996; accepted in revised form 30 July 1997

Key words: Cimmerian, paleomagnetism, Tethys, Turkmenistan

Abstract

Calc-alkaline volcanic deposits from the south-west of the Turan plate, near the city of Turkmenbasi (40°00′N, 52°58′E) in Turkmenistan, were studied paleomagnetically. These rocks have been affected by a greenschist-facies metamorphism, possibly of regional extent, that has been K/Ar-dated as 200 to 227 Ma old. A low-blocking-temperature component (D = 349°, I = 64°), close to the present field direction and probably of viscous or recent chemical origin, was isolated by a negative fold test at three sites.

The mean direction of a high-blocking-temperature component isolated at 15 sites, mainly carried by magnetite, is scattered before and after tectonic correction and is therefore difficult to interpret. A group of seven sites with low inclinations before and after tectonic correction was isolated. The mean inclination of these sites (31 ± 8°), syn-folding or post-folding, corresponds to a paleolatitude of 17 ± 8° which is lower than the conventional Eurasian paleolatitudes for post-Permian times. The paleomagnetic data from the Turan and Iran plates constrain this low paleolatitude to the Late Triassic and Jurassic period. This requires a shortening of at least 7° between the Turan plate and Eurasia during this time.

Introduction

It is generally agreed that the Turan plate, now delimited to the south by an ophiolitic belt in the Alborz range (Figure 1; Stöcklin 1974, Alavi 1991), collided with the East European craton during Carboniferous or Permian times (Zonenshain et al. 1990, Snyder et al. 1994). On paleogeographic maps for the end of the Paleozoic and the Mesozoic, this Turan plate is shown as a part of stable Eurasia, with the Paleotethys, to the south, separating it from Gondwanan microblocks such as Iran (Dercourt et al. 1993, Van der Voo 1993). According to Stöcklin (1968, 1974), Weber-Diefenbach et al. (1986), Alavi (1991) and Baud et al. (1991), the geological data show that the collision of Iran with the Turan plate began during the Late Triassic or the Early Jurassic, corresponding to the first Cimmerian folding. From a paleomagnetic standpoint (Wensink 1981, Wensink & Varenkamp 1980), the Iran plate was a part of Gondwana during the Permian, probably until the Triassic. It then drifted away from Gondwanaland to join Eurasia. During the Cretaceous its northern part was at about its present location relative to Eurasia. Supposing that Iran formed part of stable Eurasia during the Jurassic, the Early Jurassic paleomagnetic result from the Alborz (Wensink 1982) is far from that expected if compared with the expected latitude derived from the apparent polar wander path of Eurasia (Westphal et al. 1986, Besse & Courtillot 1991, Van der Voo 1990, Beck 1994). Nevertheless, the large difference of latitude could be explained by the early stage of the collision, but this hypothesis could not be checked, until now, with paleomagnetic results because the data from the Turan plate were rather scarce. The

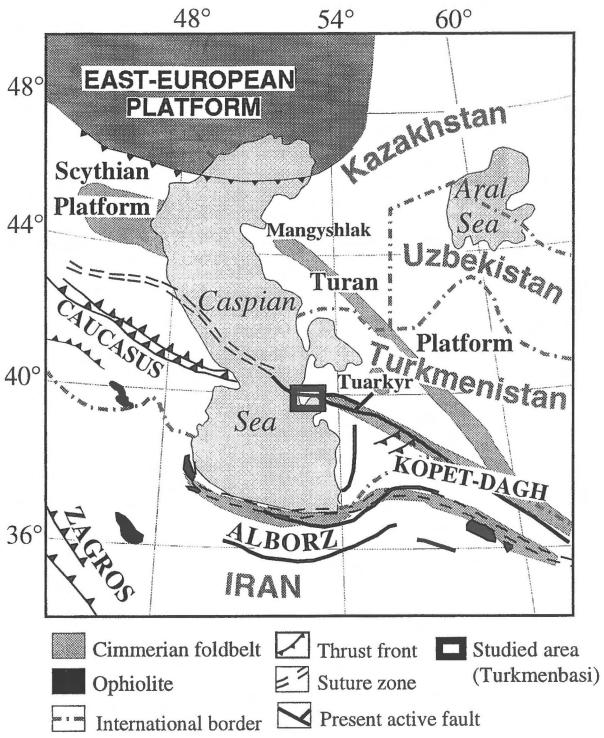

Figure 1. Schematic map of the study area and adjoining regions, after Zonenshain et al. (1990) and Erteleva et al. (1994).

results presented here, from the south-west of Turkmenistan, constrain the final shortening between the north of the Iran plate and Eurasia to Jurassic times.

Geological setting and sampling

The studied volcanic rocks crop out within an exhumed and eroded anticlinal fold on two peninsulas in the south-west of Turkmenistan, near the city of Turkmenbasi (40°00′N, 52°58′E), formerly called Krasnovodsk, (Figure 2). An angular unconformity is visible between these volcanics and the overlying Middle Jurassic sediments. On geological maps, the volcanism on the peninsulas of Turkmenbasi and Ufra, hereafter simply referred to as Turkmenbasi and Ufra, is said to date back to the Late Carboniferous to Triassic periods (Krimous et al. 1989) and to include also Early Devonian to Early Carboniferous intrusive rocks. However, no details about these age determinations can be found, and Garetsky et al. (1982), Zonenshain et al. (1990) and Khain (1977, in Malushin 1987) consider these volcanics to form the basement of the Turan platform which is now covered by Jurassic, Cretaceous and Cenozoic deposits.

A total of 21 sites were sampled, each having a surface area of at least 20 m^2, and forming an independent volcanic unit. The sites are several hundred metres to several kilometres from each other. Their location was determined with a Global Positioning System (GPS) receiver.

Petrography

The study of 22 polished thin sections in transmitted and reflected light is still in process but preliminary analyses show that the lavas and the pyroclastic rocks are acidic, heterogeneous and porphyritic, and commonly altered to greenschist metamorphic grade. In transmitted light, slightly altered quartz, more or less saussuritized feldspars, calcite, epidote and secondary quartz are present. The pyroxenes are replaced by chlorite, and veins of calcite, quartz, epidote and opaques are common. In reflected light, magnetites or titanomagnetites (which are difficult to distinguish) occur. Some titanomagnetites are finely subdivided by ilmenite lamellae. Other opaques present include ilmenites, pyrrhotites, iron oxyhydroxides, hematites and titanites. The opaque minerals, from one slide to another, are very variable in distribution, size and composition. The opaques content varied from < 1 to 5%, and the grain-size from <1 to 600μm. Differences in the degree of alteration of the opaque minerals were also observed. The current evidence suggests that a regional metamorphism may have affected the rocks of Turkmenbasi and Ufra.

Geochemistry

Different volcanic deposits were selected in order to determine their geochemical composition, and to date them using the whole-rock K/Ar technique. The geochemical analysis of eight samples, representative of seven different deposits, shows that the acidic part of the volcanic series has been sampled. The major-element content enables to classify this volcanism as high-potassium calc-alkaline, comprising rhyolites, dacites and trachytes (Figure 3). The major, trace and rare-earth element contents (Table 1), are similar to those of the active volcanic arc of Taupo in New Zealand (Carmichael et al. 1974). The observed enrichment in Ba, relative to rare-earth elements (REE), e.g.

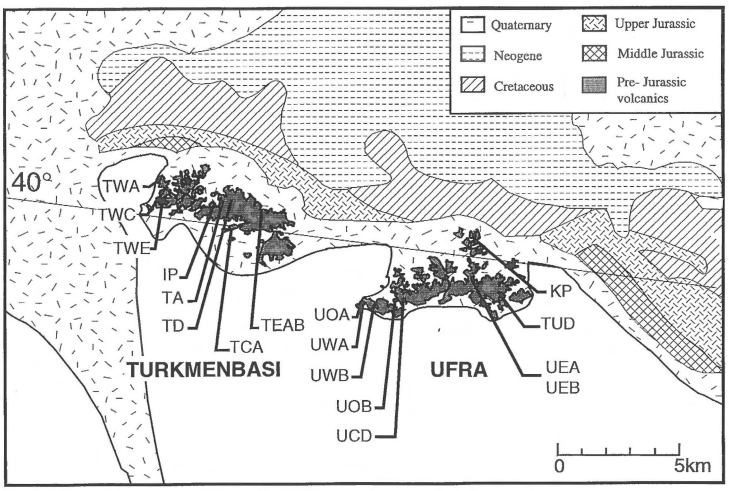

Figure 2. Schematic geological map showing the sampling sites, after Krimous et al. (1989).

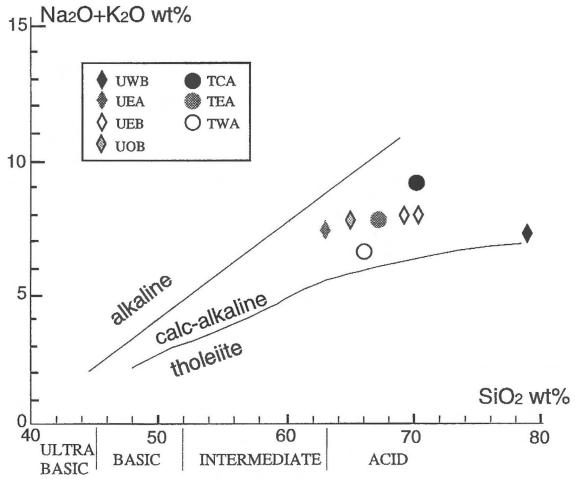

Figure 3. Alkaline-silica diagram (adapted from Brousse 1971) showing the acidic composition of seven samples.

the Ba/La ratio, is also characteristic of island arcs (Basaltic Volcanism Study Project 1981). The dating of six different deposits provided rather consistent results around 200Ma, with one sample slightly older at 227Ma (Table 2). These ages are interpreted as representing the age of the metamorphism that, on the basis of the petrological study, appears to be regional in character. As the collision of Iran with the Turan plate began at the end of the Triassic (Baud et al. 1991), this metamorphism may be related to an accretion and collision process.

Paleomagnetic analysis

Measurements

The natural remanent magnetization (NRM) of the volcanic rocks was measured in the Strasbourg laboratory, using a modified Digico spinner with a noise level of 30 μA/m. Thermal demagnetization was preferred because parasitic magnetizations were observed during alternating-magnetic-field demagnetization above an 80 mT peak applied field. Fourteen heating steps were made up to 590–600°C, with low-field susceptibilities measured every two steps, using a Digico susceptibility bridge, in order to detect any mineral transformation. Principal component analysis (Zijderveld 1967, Kirschvink 1980, Kent et al. 1983) and Fisher statistics (Fisher 1953) were used to determine the average direction for each site. The magnetic minerals were investigated using the acquisition curves of isothermal remanent magnetization (IRM) in direct magnetic fields up to 600 to 915 mT, and by continuous thermal demagnetization. The different coercivity fractions of IRM were remagnetized along two orthogonal directions (915 mT along the vertical, and 150 mT along the horizontal axis). These were then plotted separately, following Lowrie (1990), in order to identify the ferromagnetic minerals content of the rock.

Rock magnetism

Rock-magnetic investigations were performed on at least one specimen per site. In samples in which most of

Table 1. Major, trace and rare-earth elements analyses of seven different volcanic deposits from Turkmenbasi and Ufra.

Sample or site	TEAB	TWA	TCA	UEA03	UEB08a	UEB08b	UWB6-7	UOB
Major elements (wt %)								
SiO_2	67.100	66.600	69.400	63.100	68.600	69.400	78.600	64.600
Al_2O_3	14.200	14.900	14.700	16.500	14.300	15.000	10.100	16.500
MgO	1.010	0.810	0.760	1.710	0.800	1.080	0.200	1.490
CaO	2.100	3.100	1.600	3.200	1.500	1.600	0.400	2.090
Fe_2O_3	4.000	5.500	2.900	4.900	2.800	3.200	1.000	4.600
Mn_3O_4	0.127	0.159	0.064	0.117	0.132	0.170	0.017	0.109
TiO_2	0.670	0.570	0.570	0.690	0.280	0.340	0.100	0.630
BaO	0.110	0.100	0.120	0.100	0.170	0.210	0.200	
P_2O_5	0.340	0.270	0.200	0.240	0.210	0.230	0.100	0.180
SrO	0.030	0.040	0.030	0.050	0.060	0.050	0.010	
Na_2O	4.500	4.370	3.710	4.360	4.250	4.240	2.470	4.040
K_2O	2.940	2.200	4.540	2.940	3.520	3.540	3.460	3.810
Trace elements (ppm)								
Sr	264.000	361.000	266.000	429.000	470.000	462.000	123.000	441.000
Ba	994.000	890.000	1025.000	827.000	1529.000	1726.000	1773.000	1058.000
V	24.200	3.400	30.200	98.000	31.300	34.800	5.500	74.000
Ni	2.000	2.000	126.000	3.000	3.000	3.000	4.000	4.000
Co	3.700	2.400	3.700	7.800	3.100	3.400	1.100	8.000
Cr	9.700	5.800	4.300	8.600	0.400	1.100	4.900	8.000
Zn	111.000	103.000	65.000	88.000	86.000	114.000	15.000	55.000
Cu	8.000	8.000	14.000	22.000	27.000	25.000	11.000	8.000
Sc	14.200	19.000	9.200	10.500	3.900	3.900	2.900	10.000
Zr	320.000	422.000	282.000	165.000	195.000	216.000	68.000	241.000
Mn	917.000	1192.000	485.000	855.000	988.000	1194.000	116.000	
Rare earth elements (ppm)								
Rb	71.549	66.307	122.910	78.115	93.540	90.601	87.167	94.508
Y	38.475	34.429	28.588	18.816	17.915	18.111	13.127	19.924
La	34.678	39.024	43.250	29.212	48.127	56.969	29.637	29.191
Ce	72.759	77.576	85.009	55.713	84.678	99.211	54.700	56.984
Pr	8.997	9.157	9.722	6.237	8.662	10.212	5.584	6.304
Nd	36.242	35.262	36.014	22.914	28.290	33.130	18.616	23.245
Sm	7.638	7.110	6.578	4.326	4.263	4.829	3.132	4.188
Eu	2.085	2.298	1.541	1.360	1.098	1.242	0.652	1.090
Gd	6.600	6.087	5.449	3.489	3.227	3.626	2.573	3.572
Tb	1.122	1.006	0.859	0.565	0.477	0.513	0.386	0.538
Dy	6.990	6.364	5.407	3.523	2.945	3.105	2.349	3.184
Ho	1.485	1.355	1.131	0.708	0.646	0.662	0.490	0.681
Er	3.966	3.672	3.112	1.960	1.891	1.919	1.406	1.836
Tm	0.679	0.616	0.526	0.339	0.337	0.342	0.242	0.328
Yb	3.992	3.769	3.248	2.126	2.093	2.135	1.566	1.999
Lu	0.600	0.579	0.492	0.321	0.327	0.340	0.241	0.313
Hf	8.429	10.425	8.685	4.947	5.639	6.327	2.484	4.828
Th	12.201	13.337	20.409	11.303	26.681	29.360	14.878	11.107
U	2.202	3.534	4.324	2.553	6.179	6.202	1.903	2.357
Ratios								
Ba/La	27.101	22.806	23.700	23.810	31.770	30.297	59.824	36.244
Rb/Sr	0.271	0.184	0.462	0.182	0.200	0.196	0.709	0.214

the magnetization appeared to be carried by magnetite, three different behaviours could be distinguished: i) magnetite alone (Figure 4), ii) hematite and magnetite (Figure 5), and iii) titanomagnetite (Figure 6). These classifications correspond with the thin-section reflected-light observations, which indicate respectively: i) regularly distributed large, 200 to 300-μm, grains of titanomagnetites containing fine ilmenite lamellae,

Table 2. K/Ar dating of volcanic rocks from Turkmenbasi and Ufra (whole rock). The petrographic nomenclature is based on the classification of Le Bas & Streckeisen (1991).

Sample or site	Petrographic type	K_2O (wt %)	$\frac{100 rad^{40}Ar}{Total^{40}Ar}$	$rad^{40}Ar$ (10^{-11} mol/g)	Age (Ma)
UEA03	trachyte	2.936	96.9	86.44	193.7 ± 4.4
UEB08	dacite-rhyolite	3.543	95.8	110.74	205.0 ± 3.0
UWB06–07	rhyolite	3.482	97.1	103.36	195.2 ± 2.9
TWA	dacite	2.222	96.6	77.32	226.8 ± 5.2
TEA	dacite	2.936	97.6	87.21	195.3 ± 4.5
TCA	rhyolite	4.535	97.9	141.43	204.6 ± 3.0

wt.%: weight percentage.

Table 3. Low-blocking-temperature components (200–250° C) of two sites from Turkmenbasi (TWE, TEAB) and one from Ufra (KP).

Site	N	Before tectonic correction				After tectonic correction			
		Dg	Ig	kg	$\alpha_{95}g$	Ds	Is	ks	$\alpha_{95}s$
TWE	5	336	55	65	9	233	46	65	9
TEAB	19	345	68	22	7	42	45	22	7
KP	7	10	66	26	12	161	27	26	12
Mean	3	349	64	59	16			2	83

N: number of directions used for the Fisher statistics; D: declination; I: inclination; k: scattering; α_{95}: angle of 95% confidence. Suffixes g and s relate to geographic and stratigraphic coordinates, respectively.

ii) small, 5 to 10-μm, irregularly distributed grains showing alteration to hematite, and iii) heterogeneous, irregularly distributed and altered opaque minerals that may be titanomagnetites and iron oxyhydroxides.

Results

The NRM intensities range from 10 mA/m to 10 A/m among the 21 sites sampled, but within each site, the intensity is more homogeneous and varies only by a factor 1 to 20. These variations, from one site to another and within each site, are understandable in view of the heterogeneous distribution of the opaque minerals observed in thin sections. Moreover, most of the sites are in pyroclastic rocks. The NRM is usually completely demagnetized at a temperature of 600°C (Figure 7), but a low-blocking-temperature component is removed at 200–250°C in a third of the samples. This low-blocking-temperature component is often scattered, mainly due to differences in declination; the inclinations remain close to 60°. Despite this general scatter, three sites appear to have a consistent low-coercivity component (Table 3). A fold test on these sites which was clearly negative, indicates that the low-blocking-temperature component is a post-folding component, probably of viscous or recent chemical origin. Its direction (Dg = 349°, Ig = 64°) is close to the present field direction (D = 0°, I = 59°).

The high-blocking-temperature component is quite well defined for 15 sites (Table 4, Figure 8). Except sites UEA and UEB (these are very close, and grouped together as UEAB), where this low-blocking-temperature component is removed below 550°C, the NRM is generally removed at 580–600°C (Figure 7). The scatter of these site directions before and after tectonic correction means that the full fold test is inconclusive, and similar scatters during progressive unfolding suggest that there has been no synchronous remagnetization. Unfortunately the mean direction of site UEAB was too inadequately defined to perform a reliable reversal test (Figure 9). Nevertheless, the test yielded a positive, class C result (McFadden & McElhinny 1990), indicating that this site had not been remagnetized completely. Therefore, the low inclination for site UEAB, 31 ± 8° after, and 37 ± 8° before tilt correction (Table 4), could be syn- or pre-folding.

In this preliminary analysis, the variations in declination have been assumed to be of tectonic origin. The tilt corrections have a larger effect on inclinations from

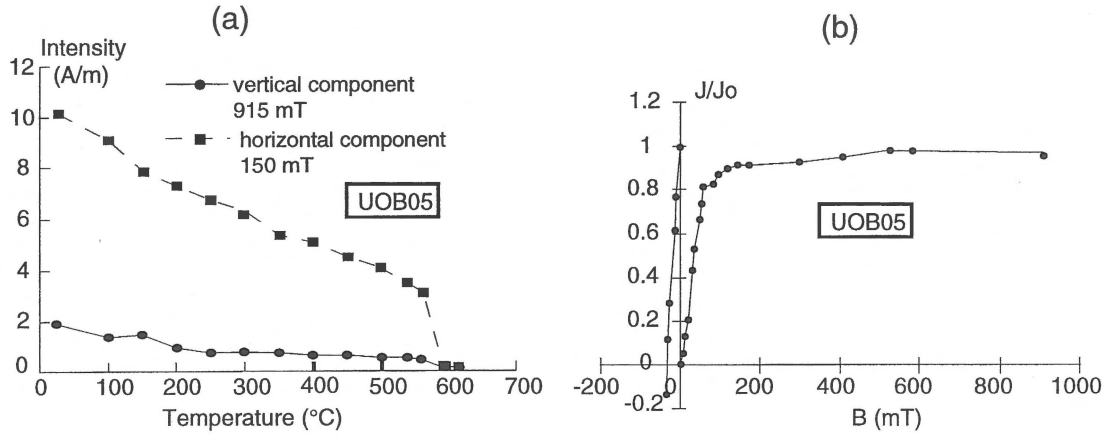

Figure 4. Rock magnetism for a sample from Ufra (UOB): a) progressive acquisition of IRM, b) thermal demagnetization of a two component IRM by magnetizing the same sample in 915 mT along its z-axis, followed by 150 mT along a horizontal axis.

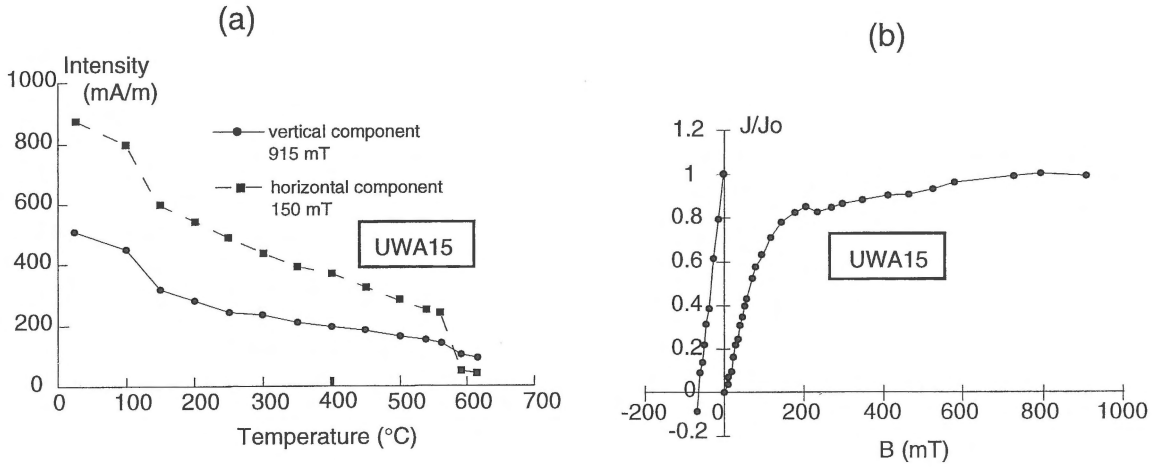

Figure 5. Rock magnetism for a sample from Ufra (UWA): for explanations see Figure 3.

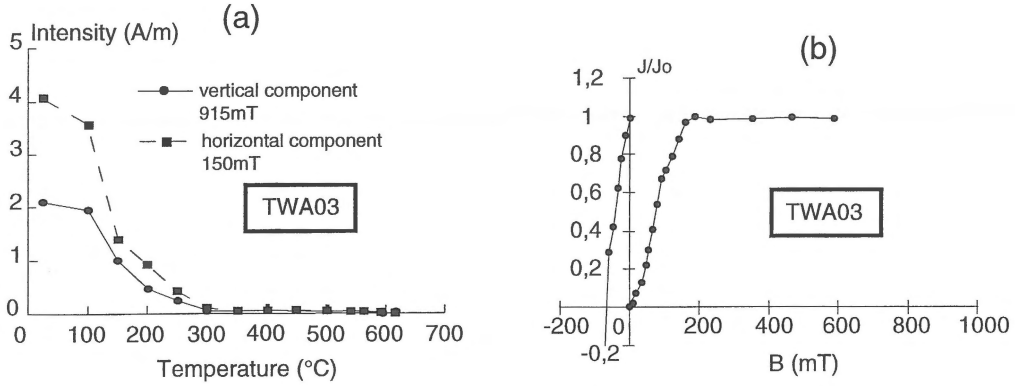

Figure 6. Rock magnetism for a sample from Turkmenbasi (TWA): for explanations see Figure 3.

Table 4. High-blocking-temperature components (for explanations see Table 3).

Site	N	Before tectonic correction				After tectonic correction			
		Dg	Ig	kg	α_{95}g	Ds	Is	ks	α_{95}s
Turkmenbasi									
TWA	13	62	33	55	6	144	55	55	6
40°01.3′N–52°55.7′E									
TWC	6	80	50	38	11	166	34	38	11
40°01.2′N–52°55.9′E									
TWE	9	42	51	18	12	164	61	18	12
40°01′N–52°55.9′E									
IP	13	75	68	202	3	100	13	202	3
40°00.7′N–52°57′E									
TA	9	23	39	265	3	72	52	265	3
40°00.7′N–52°57.1′E									
TD	9	59	49	44	8	133	57	44	8
40°00.7′N–52°57.8′E									
TEAB	23	97	59	86	3	86	21	86	3
40°00.8′N–52°58.1′E									
TCA	8	332	77	112	5	23	33	112	5
40°00.5′N–52°57.1′E									
Ufra									
UWA	8	76	33	46	8	99	29	46	8
39°58.4′N–53°03.3′E									
UWB	5	79	29	68	9	102	24	68	9
39°58.5′N–53°03.3′E									
UOA	8	88	43	23	12	115	29	23	12
59°58.5′N–53°03.02′E									
UOB	9	80	18	53	7	93	25	53	7
39°59′N–53°03.5′E									
UCD	10	90	25	84	5	104	33	84	5
39°59′N–53°03.6′E									
UEAB (UEA+UEB)	20	39	37	15	8	55	31	15	8
39°59.8′N–53°06.4′E									
TUD	8	88	32	62	7	73	1	62	7
39°59.5′N–53°07.3′E									
Mean									
Turkmenbasi + Ufra	15	69	45	11	11			6	16

Turkmenbasi, than on those from Ufra which remain low (Figure 10). But the best grouping for the results from Ufra is found before tectonic correction: I = 31 ± 8° , suggesting that this component is syn- or post-folding.

Discussion

The paleomagnetic results obtained on volcanic rocks from Turkmenbasi and Ufra are interesting but difficult to understand. The scatter of the high-blocking-temperature component is not confined to declinations alone, yet the inclinations from Ufra are consistently low and differ from those from Turkmenbasi, 7 km away. However, the results from Turkmenbasi are more complex than those from Ufra, and are still being examined. The dispersion in the Ufra declinations is probably associated with regional and local tectonics connected to the Ashkhabat fault. The mean inclination of 31 ± 8° is considered to be of post-folding or syn-folding origin. It corresponds to a paleolatitude of 17 ± 8°. The main problem now is to assess the age of this secondary magnetization. The petrographic obser-

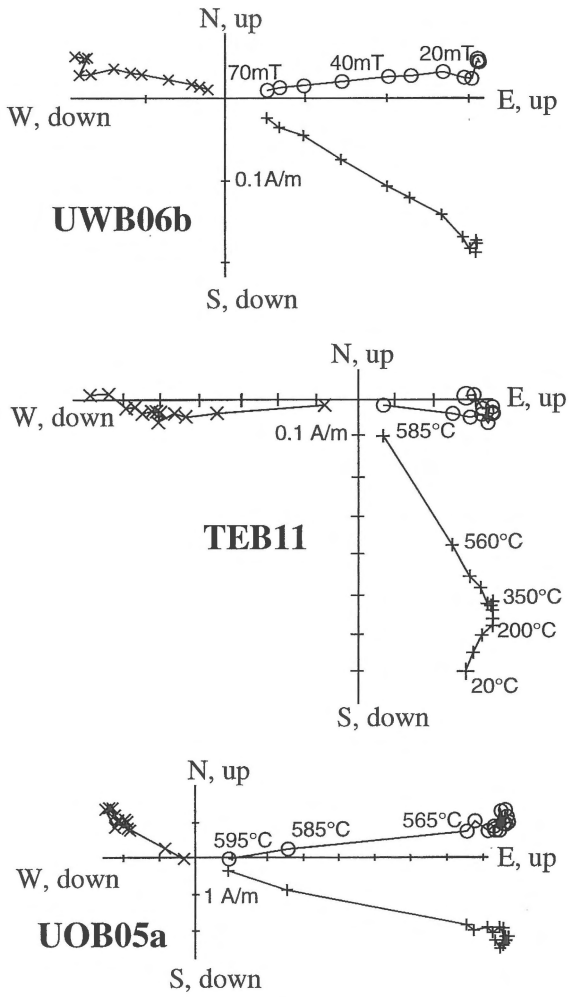

Figure 7. Curves of demagnetization. Examples of two samples from Ufra (UOB and UWB) and one from Turkmenbasi (TEB), with a high-blocking-temperature component. o: horizontal plane; +: E-W vertical plane; x: N-S vertical plane.

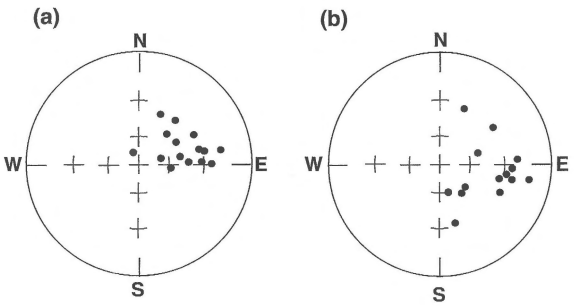

Figure 8. Mean directions for 15 sites from Turkmenbasi and Ufra: a) before, b) after tectonic correction.

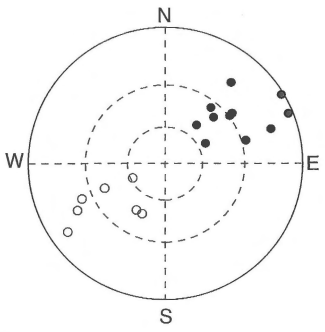

Figure 9. Reversed (○) and normal (●) directions from sites UEA and UEB (grouped as UEAB) in stratigraphic coordinates. The reversal test (McFadden & McElhinny 1990) is classified C.

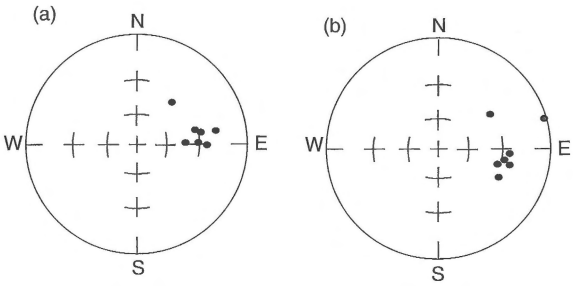

Figure 10. Mean directions for the seven sites from Ufra. a) before, b) after tectonic correction.

vations suggest that a regional greenschist-facies metamorphism affected both peninsulas. It can be assumed that the related mineral transformations had an effect on both the age determinations and the magnetization directions. Consequently, the radiometric ages probably correspond to the age of metamorphism, extending over more than 30Myr (195–227Ma) and coinciding with the beginning of the collision and the accretion of the Iran plate on the Turan plate, i.e. this complex process began at the end of the Triassic or the beginning of the Jurassic. The low inclination is most likely associated with the last stages of this metamorphism or with later events, i.e. it was acquired less than 227Ma ago.

Comparison of this direction with other results from the southern part of the Turan plate for the Jurassic and the Cretaceous is uncertain as most of the data are of poor reliability (Table 5). The most reliable are those of Bazhenov (1987) as these are based on both thermal treatment and positive fold tests, although even these directions are not all primary. Nonetheless, the corresponding paleolatitudes can be compared (Figure 11) with those expected by extrapolation from those for Eurasia (Beck 1994). The paleolatitude (plat.) for the

Table 5. Compilation of paleomagnetic results from the southern part of the Turan plate and from the northern part of the Iran plate from Late Triassic to Cretaceous times. The paleolatitudes were calculated at the reference point of Turkmenbasi.

Age (Ma)	Location	NbS	Nbs	Treatment	Tests	Pole position		Turkmenbasi		Reference
						lat.	long.	plat.	dplat	
Turkmenistan										
195–227	40°N–53°E	7	68	T	Rc			17°	8°	this paper
157–178	40°N–54°E	215	215	T	N	76°N	225°E	26°	3°	M1016
157–164	41°N–56°E	33	68	T	N	74°N	109°E	47°	2°	M1016
112–125	39°N–55°E	11	22	N	F+, Ro	60°N	167°E	24°	6°	M877
90–125	38.5°N–56.5°E	12	125	T	N	74°N	145°E	36°	4°	M1974
90–120	39°N–56°E	8	101	T	F+	75°N	153°E	36°	5°	Bazhenov
56– 89	38.5°N–56.5°E	7	162	T	F+	74°N	193°E	27°	2°	M1966
83– 88	40°N–54°E		142	A, V	N	80°N	166°E	36°	2°	M871
Iran										
178–235	35.7°N–52.3°E	5	21	A, T	N	49°N	153°E	24°	4°	M1937, W.
185–200	33°N–57°E	20		A, T		38°N	314°E	18°	7°	S. & F.
160–200	33°N–57°E	3		A, T		15°N	349°E	22°	22°	S. & F.
145–155	34°N–57°E	4	48	T	Fo	79°N	217°E	30°	11°	M1503, W.
Cretaceous	36.3°N–51.8°E	20	140	A, T	N	61°N	147.5°E	32°	7°	W. & V.

NbS: number of sites, Nbs: number of samples. Treatment: A: alternative field, T: thermal, V: viscosity. Tests: Fo: inconclusive fold test, F+: positive fold test, N: no test, Ro inconclusive reversal test, Rc: positive reversal test classified C according to McFadden & McElhinny (1990). lat.: latitude, long.: longitude, plat.: paleolatitude, dplat.: confidence limit on the paleolatitude. References: M1016: Lock & McElhinny (1991) data base, reference number 1016; Bazhenov (1987); W.: Wensink (1982); W. & V.: Wensink & Varenkamp (1980); S. & F.: Soffel & Förster (1980).

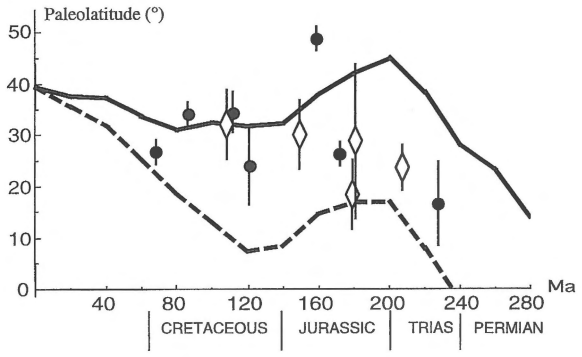

Figure 11. Theoretical and measured paleolatitudes for the Turan plate at the Turkmenbasi point of reference. The solid and dashed lines show the theoretical paleolatitude curves for Eurasia and Africa respectively, calculated from synthetic apparent polar wander paths (Beck 1994).: ◇ : Iranian data, • : Turkmenistan data.

new Ufra results, 17 ± 8° , is well below this curve. While it can be assumed that Bazhenov's data (plat. = 36 ± 5°) are from rocks not older than Middle Cretaceous (Aptian to Cenomanian), the age of the Ufra paleolatitude is constrained to the period from Late Triassic to Early Cretaceous. This requires a shortening between the Turan and Eurasian platforms of some 10°. At that time the Turan plate was lying north of the Iranian plate. A comparison with results from the Alborz range in northern Iran for the Late Triassic to the Middle Cretaceous (Table 5, Figure 11) suggests that the Ufra paleolatitude is more likely to be of the same age as the Alborz data for the Late Triassic-Early Jurassic. Consequently, the smallest shortening is 7° between Turan and Eurasia, and 3° between Iran and Turan. Although the most impressive known tectonic movements seem to be in Iran and in the south of Turkmenistan, the largest difference of latitude is obtained between Eurasia and Turan, and not between Turan and Iran. This could be due to imprecision in the Eurasian Jurassic poles, as Bazhenov et al. (1996) suggested, or, as hypothesised by Bratash (1975), the southern margin of the Turan plate could be allochthonous.

Acknowledgements

Financial support was given by the Peri-Tethys program (94-27), the International Association for the promotion of cooperation with scientists from the independent states of the former Soviet Union (INTAS, 94-3036), and the Centre National de la Recherche Scientifique (CNRS; MDRI). Geochemical analysis

and K-Ar age determinations were made by the Centre de Géochimie de la Surface (CNRS-UPR 6251 Strasbourg). We thank B.M. Honnorez and J. Honnorez who kindly examined thin sections of volcanic rocks from Turkmenbasi. We thank H. Wensink for his critical comments, and an anonymous reviewer for his linguistic help. This is a contribution of CNRS, UMR 7516 and URA 1316.

References

Alavi M. 1991 Sedimentary and structural characteristics of the Paleo-Tethys remnants in northeastern Iran – Geol. Soc. of Amer. Bull. 103: 983–992

Basaltic Volcanism Study Project 1981 Basaltic Volcanism on the Terrestrial Planets. Pergamon Press, Inc., New York, 1286 pp

Baud A., G. Stampfli & D. Steen 1991 The Triassic Aghdarband Group: Volcanism and Geological Evolution – Abh. Geol. B.-A. 38: 125–137

Bazhenov M.L. 1987 Paleomagnetism of Cretaceous and Paleogene sedimentary rocks from the Kopet-Dagh and its tectonic implications – Tectonophysics 136: 223–235

Bazhenov M.L., V.S. Burtman & N.L. Levashova 1996 Lower and Middle Jurassic paleomagnetic results from the south Lesser Caucasus and the evolution of the Mesozoic Tethys ocean – Earth Planet. Sci. Lett. 141: 79–89

Beck F. 1994 Courbes de dérive des pôles du Permien à l'actuel pour les continents péri-atlantiques et indiens. Thèse Doctorat, Strasbourg, 215 pp

Besse J. & V. Courtillot 1991 Revised and Synthetic Apparent Polar Wander Paths of the African, Eurasian, North American and Indian Plates, and True Polar Wander since 200Ma – J. Geophys. Res. 96: 4029–4050

Bratash V.I. 1975 Kerman-Kashmer trough, Iran, and the problem of the junction between pre-Jurassic structures of the Turanian plate and the Mediterranean belt – Geotectonics 9: 101–107

Brousse R. 1971 Magmatologie du volcanisme néogène et quaternaire du Massif Central – 'Symposium J. Jung', Plein-Air Service, Clermont-Ferrand: 377–478

Carmichael I.S.E., F.J. Turner & J. Verhoogen 1974 Igneous Petrology. McGraw-Hill, New York. 739 pp

Dercourt J., L.E. Ricou & B. Vrielynck (eds) 1993 Atlas Tethys Palaeoenvironmental Maps. Gauthier-Villars, Paris, 307 pp, 14 maps, 1 pl.

Erteleva O.O., S.L. Yunga & M.A. Danilova 1994 Mass identification of earthquake source mechanisms in Kopetdag seismic zone – Physics Solid Earth 30: 46–54

Fisher R.A. 1953 Dispersion on a sphere – Proc. Roy. Soc. 217A: 295–305

Garetsky R.G., A.E. Chlesinger & A.L. Ianchin 1982 Les plateformes épi-paleozoîques du Sud de la plate-forme de l'Europe de l'Est: Plate-forme du Touran. In: Peive A.V., V.E. Khain., M.V. Mouratov & F. Delany (eds) Tectonics of Europe and Adjacent Areas: Variscides, Epi-Paleozoïc Platforms, Alpides 2. Nauka Publishing House, Moscow: 254–269

Kent D.V., J.C. Briden & K.W. Mardia 1983 Linear and planar structure in ordered multivariate data as applied to progressive demagnetization of palaeomagnetic remanence – Geophys. J. R. astr. Soc. 75: 593–621

Khain V.Y. 1977 Regional'naya geotektonika (Vneal'piyskaya Yevropa i zapadnaya Aziya) (Regional geotectonics. Extra-Alpine Europe and western Asia). Moscow, Nedra. 359 pp

Kirschvink J.L. 1980 The least square line and plane and the analysis of paleomagnetic data – Geophys. J. R. astr. Soc. 62: 699–718

Krimous V.N., E.P. Abrosimova, V.P. Kalougin, N.N. Kamichev, B.A. Krasilnikov, L.V. Kornienko, I.N. Loukin, N.F. Melnikova, M.S. Pachaev & M.A. Popova 1989 Geological Map of Turkmenistan: 1:500 000. U.S.S.R.

Le Bas M.J. & Streckeisen A.L. 1991 The IUGS systematics of igneous rocks - J. Geol. Soc. London 148: 825–833

Lock J. & M.W. McElhinny (eds) 1991 The global paleomagnetic database; design, installation and use with ORACLE – Surveys Geophys. 12: 317–505

Lowrie W. 1990 Identification of ferromagnetic minerals in rocks by coercivity and unblocking temperature properties – Geophys. Res. Lett. 17: 159–162

Malushin I.I. 1987 The Caspian-Turanian Paleomega-Arch and Related Southern Continental Rift System – Geotectonics 21: 137–142

McFadden P.L. & M.W. McElhinny 1990 Classification of the reversal test in paleomagnetism – Geophys. J. Int. 103: 725–730

Snyder W.S., C. Spinosa, V. I. Davidov & P. Belasky 1994 Petroleum Geology of the Southern Pre-Uralian Foredeep with Reference to the Northeastern Pre-Caspian Basin – Int. Geol. Rev. 36: 452–472

Soffel H.C. & H.G. Förster 1980 Apparent Polar Wander path of Central Iran and its Geotectonic Interpretation – J. Geomag. Geoelectr. 32: SIII 117–SIII 135

Stöcklin J. 1968 Structural history and tectonics of Iran: a review – Am. Ass. Petrol. Geol. Bull. 52: 1229–1258

Stöcklin J. 1974 Possible Ancient Continental Margin in Iran. In: Burk C.A. & C.L. Drake (eds) The geology of continental margins. Springer, Berlin: 873-887

Van der Voo R. 1990 Phanerozoic paleomagnetic poles from Europe and north America and comparisons with continental reconstructions – Rev. Geophys. 28: 167–206

Van der Voo R. 1993 Paleomagnetism of the Atlantic, Tethys and Iapetus Oceans. University Press, Cambridge. 411 pp

Weber-Diefenbach K., M. Davoudzadeh, N. Alavi-Tehrani & G. Lensch 1986 Paleozoic ophiolites in Iran. Geology, geochemistry and geodynamic implication – Ofioliti 11: 305–338

Wensink H. 1981 Le contact Gondwana-Eurasie en Iran d'après les recherches paleomagnétiques – Bull. Soc. géol. France 6: 547–552

Wensink H. 1982 Tectonic Inferences of the Paleomagnetic Data from some Mesozoic Formations in Central Iran – J. Geophys. 51: 12–23

Wensink H. & J.C. Varenkamp 1980 Paleomagnetism of basalts from Alborz: Iran part of Asia in the Cretaceous – Tectonophysics 68: 113–129

Westphal M., M.L. Bazhenov, J.P. Lauer, D.M. Pechersy & J.C. Sibuet 1986 Paleomagnetic implications and evolution of the Tethys belt from Atlantic Ocean to the Pamirs since Triassic – Tectonophysics 123: 37–82

Zijderveld J.D.A. 1967 Demagnetization: analysis of results. In: Collinson D.W., K.M. Creer & S.K. Runcorn (eds) Methods in Paleomagnetism. Elsevier: 254–286

Zonenshain L.P., M.I. Kuzmin & L.M. Natapov 1990 Geology of the USSR: A Plate-Tectonic Synthesis. Geodynamic Series 21, Amer. Geophys. Union, Washington, DC. 242 pp